



Wave based method for vibration and acoustic characteristics analysis of underwater cylindrical shell with bulkheads

Kun Xie¹; Meixia Chen²; Naiqi Deng³; Kun Xu⁴

^{1, 2, 3, 4} Huazhong University of Science and Technology, China

ABSTRACT

Wave based method (WBM) is presented to analyze the vibration and acoustic responses of underwater cylindrical shell with bulkheads under a radial harmonic excitation. The hull is divided into several substructures and the dynamic field variables in each substructure are expressed as wave function expansions. The stiffeners and bulkheads are treated as discrete members and the equations of motion of annular plate are adopted to describe the motion of them. Boundary and continuity conditions between adjacent substructures are used to form the final matrix to be solved. The far-field radiated sound pressure is then calculated by means of the Element Radiation Superposition Method (ERSM). By comparison with computational results obtained from a fully coupled finite element/boundary element model, the present method is verified. Furthermore, effects of bulkheads and location of exciting force on vibro-acoustic characteristics of cylindrical shell have been discussed. The results show that bulkhead thickness has negligible influence on the response, but the number of bulkheads, the location of bulkheads and the exciting force have significant effects.

Keywords: wave based method, stiffened cylindrical shell with bulkheads, vibration and acoustic response
I-INCE Classification of Subjects Number(s): 54.3, 75.9

1. INTRODUCTION

The cylindrical shell reinforced with ring stiffeners is widely used in structural design and the dynamic and acoustic responses of it have received much research attention. The vibration and acoustic analysis of such stiffened shells are studied either by treating stiffeners as discrete member (1, 2) or by applying “smeared out” technique (3-5). In order to accommodate various design requirements in practical engineering applications, the shell is often divided into compartments by bulkheads, which can be represented by circular plate. Ref. (6) has studied the dynamic response caused by cylinder/plate discontinuity and the analytical model in Ref. (6) can be developed to describe bulkheads. When the finite shell is submerged in heavy fluid, such as water, the fluid-loading effect has to be considered in the model of cylindrical shell (7, 8). Ref. (4, 5) discussed the influence of bulkheads and fluid-loading on the structural and acoustic responses, but the force was located at the end plate and only the modes of $n=0$ and $n=1$ were excited, which results in the conclusion that bulkheads has no significant effects on the response.

For the reason of only a small number of simple structures allowing analytical solution of the Helmholtz formulation calculating the radiated pressure from structures, many researchers have investigated approximate methods for finite cylindrical shell, such as boundary element method (9), coupled finite/boundary element method (10). Element radiation superposition method (ERSM) was proposed by Wang (11) and was based on two assumptions. The first is that the elements on radiating surface could be treated as rigid piston with a rigid cylindrical baffle as the size of elements is small enough, and the second is that the pressure of far field point is the superposition of radiated pressure from all elements. ERSM is superior in terms of computational efficiency, especially for large scale

¹ xiekun79@163.com

² chenmx26@hust.edu.cn

³ dengnq@hust.edu.cn

⁴ xukun@hust.edu.cn

structures.

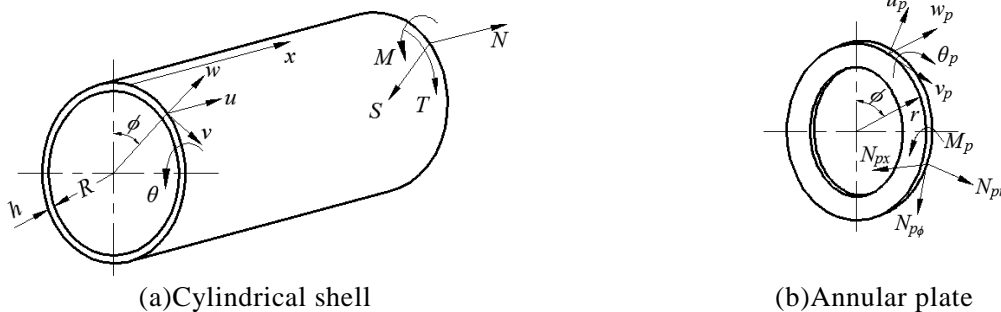
Wave based method (WBM) was proposed in Ref. (12) for prediction of the steady-state dynamic analysis of coupled vibro-acoustic systems. The field variables are expanded in terms of structural and acoustic wave functions which satisfy the dynamic equations accurately. Ref. (13) developed the WBM to analyze the free vibration characteristics of cylindrical shell with non-uniform stiffener distribution. In Ref. (13), the equations of motion of annular plate were adopted to describe the motion of stiffeners in contrast with the conventional beam model (1, 2), and an excellent agreement was obtained compared with the experimental and computational results, even though the eccentricity of stiffeners is not zero.

In this paper, WBM is developed for the dynamic analysis of underwater cylindrical shell with stiffeners and bulkheads. The hull is divided into several substructures first, such as cylindrical shells, annular plates and circular plates, then select the wave functions which accurately satisfy governing dynamic equations of the substructure, last assemble the matrix of boundary and continuity conditions at junctions and solve the matrix to obtain the vibration response, which is used to predict far-field pressure by means of ERSM.

2. THEORETICAL FORMULATIONS

2.1 Motion Equations

Stiffeners and bulkheads appear as discontinuities and divide the cylindrical shell into different substructures, such as cylindrical shells, annular plates and circular plates. Fig. 1(a) shows coordinate system, displacements and forces of cylindrical shell, u, v, w are the axial, circumferential, radial direction displacements, $\theta = \partial w / \partial x$ is the twist angle, M, S, T and N designate bending moment, transverse shear, tangential shear and axial force per unit length of the cylindrical shell, and their detailed expressions can be obtained in Ref. (14). Fig. 1(b) shows coordinate system, displacements and forces of annular plate, u_p, v_p and w_p are the in and out-plane displacements, $\theta_p = \partial w / \partial r$ is the twist angle, $N_{px}, N_{pr}, N_{p\phi}$ and M_p denote the transverse shear, radial, tangential shear force and moment per unit length of the annular plate, respectively.



(a) Cylindrical shell

(b) Annular plate

Figure 1 - Coordinate system, displacements and forces of substructures

The equations of motion for cylindrical shell can be written by Donnell-Mushtari theory as

$$\begin{aligned}
 & \left(\frac{\partial^2}{\partial x^2} + \frac{1-\nu}{2R^2} \frac{\partial^2}{\partial \phi^2} - \frac{1}{c_L^2} \frac{\partial^2}{\partial t^2} \right) u + \left(\frac{1+\nu}{2R} \frac{\partial^2}{\partial x \partial \phi} \right) v + \left(\frac{\nu}{R} \frac{\partial}{\partial x} \right) w = 0 \\
 & \left(\frac{1+\nu}{2R} \frac{\partial^2}{\partial x \partial \phi} \right) u + \left(\frac{1-\nu}{2} \frac{\partial^2}{\partial x^2} + \frac{1}{R^2} \frac{\partial^2}{\partial \phi^2} - \frac{1}{c_L^2} \frac{\partial^2}{\partial t^2} \right) v + \left(\frac{1}{R^2} \frac{\partial}{\partial \phi} \right) w = 0 \\
 & \left(\nu \frac{1}{R} \frac{\partial}{\partial x} \right) u + \left(\frac{1}{R^2} \frac{\partial}{\partial \phi} \right) v + k \left(\frac{1}{R^2} + R^2 \frac{\partial^4}{\partial x^4} + 2 \frac{\partial^4}{\partial x^2 \partial \phi^2} + \frac{1}{R^2} \frac{\partial^4}{\partial \phi^4} + \frac{1}{c_L^2} \frac{\partial^2}{\partial t^2} \right) w - F_L w = 0
 \end{aligned} \tag{1}$$

where R is the mean radius of the cylindrical shell, h is the shell thickness, E, ρ, ν are, respectively, the Young's modulus, density and Poisson's ratio of the shell, $k = h^2 / (12R^2)$ is the thickness parameter, $c_L = [E / \rho(1-\nu^2)]^{1/2}$ is the longitudinal wave speed. F_L is the fluid loading term due to the presence of the surrounding fluid acoustic field and can be approximately given in terms of a fluid-loaded infinite model (15)

$$F_L = -\Omega^2 \frac{\rho_f}{\rho} \frac{1}{R^2 h} \frac{1}{(k_f^2 - k^2)^{1/2}} \frac{H_n((k_f^2 - k^2)^{1/2} R)}{H_n'((k_f^2 - k^2)^{1/2} R)} \quad (2)$$

where $\Omega = \omega R/c_L$ is non-dimensional circular frequency, ω is circular frequency and ρ_f is the density of fluid. H_n is the Hankel function of order n and H_n' is its derivative respect to the argument. k_f is the acoustic wave number and k is the axial wave number. When $k_f < k$ the Hankel function is replaced by a modified Hankel function K_n of real argument.

The stiffeners and bulkheads are treated as discrete members, the motions of which are described by the equations of motion of annular plate (6)

$$\begin{aligned} \nabla^4 w_p + (\rho_p h_p / D_p) \frac{\partial^2 w_p}{\partial t^2} &= 0 \\ \frac{\partial}{\partial r} \left(\frac{\partial u_p}{\partial r} + \frac{u_p}{r} + \frac{1}{r} \frac{\partial v_p}{\partial \phi} \right) - \frac{1 - \nu_p}{2r} \frac{\partial}{\partial \phi} \left(\frac{\partial v_p}{\partial r} + \frac{v_p}{r} - \frac{1}{r} \frac{\partial u_p}{\partial \phi} \right) &= \frac{\rho_p (1 - \nu_p^2)}{E_p} \frac{\partial^2 u_p}{\partial t^2} \\ \frac{1}{r} \frac{\partial}{\partial \phi} \left(\frac{\partial u_p}{\partial r} + \frac{u_p}{r} + \frac{1}{r} \frac{\partial v_p}{\partial \phi} \right) + \frac{1 - \nu_p}{2} \frac{\partial}{\partial r} \left(\frac{\partial v_p}{\partial r} + \frac{v_p}{r} - \frac{1}{r} \frac{\partial u_p}{\partial \phi} \right) &= \frac{\rho_p (1 - \nu_p^2)}{E_p} \frac{\partial^2 v_p}{\partial t^2} \end{aligned} \quad (3)$$

where $\nabla^4 = [\partial^2 / r^2 + (1/r) \partial / r + (1/r^2) \partial^2 / \phi^2]^2$, $D_p = E_p h_p / 12(1 - \nu_p^2)$. E_p , h_p , ρ_p and ν_p are the Young's modulus, thickness, density and Poisson's ratio of the plate, respectively.

2.2 Selection of Wave Functions

In the wave based method, the displacement components of the shell and annular plate are expressed as

$$u = \sum_{i=1}^{n_s} A_i \Psi_{ui} \cos(n\phi) e^{-j\omega t}, \quad v = \sum_{i=1}^{n_s} B_i \Psi_{vi} \sin(n\phi) e^{-j\omega t}, \quad w = \sum_{i=1}^{n_s} C_i \Psi_{wi} \cos(n\phi) e^{-j\omega t} \quad (4)$$

where Ψ_{ui} , Ψ_{vi} and Ψ_{wi} , which are the functions of x and r for cylindrical shell and annular plate, are the structure wave functions satisfying Eq. (1) and (2) for a particular circumferential mode number n . A_i , B_i and C_i are the wave contribution factors. n_s is the number of wave functions designing the wave propagation in the axial direction for the cylindrical shell and in the radial direction for the annular plate.

According to Ref. (1), $\Psi_{ui} = \Psi_{vi} = \Psi_{wi} = e^{jk_{n,i}x}$. Substituting Eq. (4) into (1), three linear equations in terms of A_i , B_i and C_i are obtained. For nontrivial solution, the determinant of their coefficients must vanish and a characteristic equation in terms of k_n is obtained. Eight eigenvalues are obtained by meaning of numerical method to solve the characteristic equation. For each value of $k_{n,i}$ ($i=1:8$), the axial and circumferential wave contribution facts can be obtained as $\xi_i = A_i/C_i$ and $\eta_{n,i} = B_i/C_i$, respectively, so that the eight selected wave functions of cylindrical shell are as follows:

$$\Psi_{ui} = \Psi_{vi} = \Psi_{wi} = e^{jk_{n,i}x} \quad i=1:8 \quad (5)$$

Replacing $C_{n,i}$ by $W_{n,i}$, the relationships of wave contribution factors of cylindrical shell are $A_{n,i} = \xi_{n,i} W_{n,i}$, $B_{n,i} = \eta_{n,i} W_{n,i}$ ($i=1:8$), which means n_s equals 8 for cylindrical shell.

According to Ref. (6), there are a set of wave functions to compose the variable field of annular plat:

$$\begin{aligned} \Psi_{up1} &= dJ_n(k_{pL}r)/dr, & \Psi_{up2} &= nJ_n(k_{pT}r)/r, & \Psi_{up3} &= dI_n(k_{pL}r)/dr, & \Psi_{up4} &= nK_n(k_{pT}r)/r \\ \Psi_{vp1} &= nJ_n(k_{pL}r)/r, & \Psi_{vp2} &= dJ_n(k_{pT}r)/dr, & \Psi_{vp3} &= nI_n(k_{pL}r)/r, & \Psi_{vp4} &= dK_n(k_{pT}r)/dr \\ \Psi_{wp1} &= J_n(k_{pB}r), & \Psi_{wp2} &= Y_n(k_{pB}r), & \Psi_{wp3} &= I_n(k_{pB}r), & \Psi_{wp4} &= K_n(k_{pB}r) \end{aligned} \quad (6)$$

where J_n, Y_n are, respectively, the Bessel function functions of the first and second kind, and I_n, K_n are the modified Bessel functions of the first and second kind, respectively. $k_{pB} = (\rho_p \omega^2 h_p / D_p)^{1/4}$ is the plate bending wavenumber, $k_{pL} = \omega[\rho_p(1 - \nu_p^2)/E_p]^{1/2}$ and $k_{pT} = \omega[\rho_p(1 + \nu_p)/E_p]^{1/2}$ are the wavenumber for in-plane waves in the plate. Although there seems to be 12 wave functions for annular plate from

Eq. (6), the wave functions of Ψ_{upi} and Ψ_{vpi} are essentially identical and the wave contribution factors are the same, $A_i = B_i$. As a result, n_s equals 8 for annular plate. The relationships of wave contribution factors are $A_i = B_i = A_{n,i}$, $C_i = C_{n,i}$ ($i = 1:4$).

For the circular plate, setting $A_{n,3}, A_{n,4}, C_{n,3}$ and $C_{n,4}$ to 0 and then wave functions (6) can be adopted to analyze the bulkheads and end plates in terms of stiffeners.

2.3 Boundary and continuity conditions

As shown in Fig. 1(a), the cylindrical shell has four displacement constrains (u, v, w, θ) and four force or moment constrains (M, S, T, N) at the cross section:

$$u = 0, v = 0, w = 0, \theta = 0, M = 0, S = 0, T = 0, N = 0 \tag{7}$$

Combination of these eight simple boundary conditions can present any complex ones, that is to say the present method can be adopted to analyze the vibration characteristics of cylindrical shell with arbitrary conditions. In the following analysis, the shell is closed by two end plates and the continuity conditions at the junctions of end plate and shell replace the boundary conditions.

When the stiffened shell with bulkheads is divided into several segments, the continuity equations must be satisfied. Considering the circular plate is a special case of the annular plate, without loss of generality, Fig.2 shows the displacements, forces and moments at junction of the τ th stiffener.

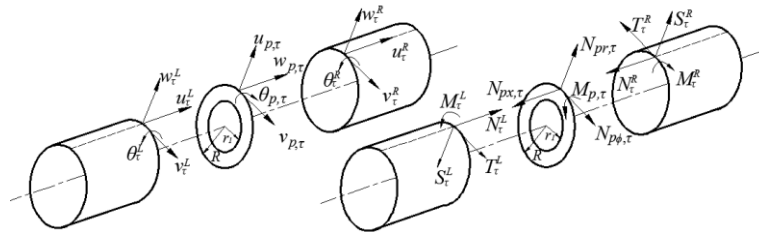


Figure 2 – Junction displacements, forces and moments

At the outer radius of the annular plate as shown in Fig. 2, the continuity conditions of displacements, forces and moments can be expressed as follows:

$$u_{\tau}^L = u_{\tau}^R = w_{p,\tau} |_{r=R}, v_{\tau}^L = v_{\tau}^R = v_{p,\tau} |_{r=R}, w_{\tau}^L = w_{\tau}^R = u_{p,\tau} |_{r=R}, \theta_{\tau}^L = \theta_{\tau}^R = -\theta_{p,\tau} |_{r=R} \tag{9}$$

$$N_{\tau}^L - N_{\tau}^R - N_{px,\tau} |_{r=R} = 0, S_{\tau}^L - S_{\tau}^R - N_{pr,\tau} |_{r=R} = 0, T_{\tau}^R - T_{\tau}^L - N_{p\theta,\tau} |_{r=R} = 0, M_{\tau}^R - M_{\tau}^L - M_{p,\tau} |_{r=R} = 0 \tag{10}$$

Subscript τ denotes the τ th stiffener, and superscript L and R denote the left and right side of the τ th stiffener, respectively.

At the inner radius of the annular plate, the boundary of the annular plate is free:

$$N_{px,\tau} |_{r=r_i} = 0, N_{pr,\tau} |_{r=r_i} = 0, N_{p\theta,\tau} |_{r=r_i} = 0, M_{p,\tau} |_{r=r_i} = 0 \tag{11}$$

Eq. (11) is only appropriate for the annular plate and it will vanish for the circular plate. Since the junction of cylindrical shell and end plate is a special case, the continuity conditions can refer to Eq. (9) to (11) and the displacements and forces of cylindrical shell on left or right side vanish.

2.4 Force excitation and frequency response function

The structural response to a point harmonic force excitation can be calculated by considering the external force as part of the boundary conditions. A radial point force, as shown in Fig. 3, is located at one junction of stiffener and cylindrical shell. Assuming the point force located at (x_0, ϕ_0) and the force can be described in terms of Dirac delta functions by

$$F = F_0 \delta(x - x_0) \delta(\phi - \phi_0) e^{-j\omega t} \tag{12}$$

where F_0 is the amplitude of external force.

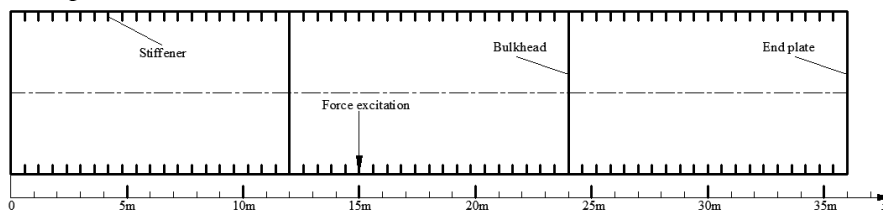


Figure 3 – Schematic diagram of stiffened shell with bulkheads

When the force is located at the junction of stiffener/bulkhead and cylindrical shell, the external force results in modification to the equilibrium of the second equation of Eq. (11), which becomes

$$S_{\tau}^L - S_{\tau}^R - N_{pr,\tau} |_{r=R} = F \tag{13}$$

When the direction of external force is axial direction or circumferential direction, the modification will occur in corresponding equilibrium in Eq. (11). Excluding the time harmonic dependency, multiplying the above equation by $\cos(n\phi)$ and taking the integral from $-\pi$ to π , Eq. (13) becomes

$$(S_{\tau}^L - S_{\tau}^R) - N_{pr,\tau} |_{r=R} = \varepsilon F_0 \cos(n\phi_0) \tag{14}$$

where $\varepsilon = 1/2\pi R$ if $n = 0$ and $\varepsilon = 1/\pi R$ if $n \neq 0$.

When the force is located at the cylindrical shell between two adjacent stiffeners, the segment of cylindrical shell needs to be divided into two segments and the continuity conditions are similar to Eq. (9), (10) and (14), but the displacements and forces of stiffener must vanish.

Assembling all the boundary and continuity conditions in the matrix form $\mathbf{B}\mathbf{x}=\mathbf{F}$, where \mathbf{B} is the matrix consisting of the expressions of displacements and forces in terms of corresponding wave contribution factors at junctions, \mathbf{x} is the vector of the unknown wave contribution factors and \mathbf{F} is the force vector with only one non-zero element corresponding to $\varepsilon F_0 \cos(n\phi_0)$. The steady state forced response of each circumferential mode number n is calculated by solving the system and the final response is the superposition of all different circumferential mode number n at the certain frequency.

2.5 Far-Field Sound Pressure

The radiating surface, without taking into account the scattering at the end plates, is divided into N elements and the far field sound pressure is the superposition of the acoustic pressures radiated from the discrete elements (11, 15):

$$p(\vec{r}) = [\mathbf{G}]_{1 \times N} [\mathbf{v}]_{N \times 1} \tag{15}$$

where \vec{r} denotes the location of the field point, $[\mathbf{v}]$ is the normal velocity vector of all elements at particular frequency, $[\mathbf{G}]$ is the acoustic transfer vector (ATV) and G_i , the i th element of matrix $[\mathbf{G}]$, represents contribution of the corresponding element to the observation field point when the i th element is the only element vibrating with unit speed and the others are at rest. The ATV depends on the considered frequency, the geometry, acoustical parameters of fluid and the position of the observation point.

As N , the total number of discrete surface elements, is large enough, the elements can be treated as rigid piston with cylindrical baffle and the far field acoustic pressure radiated from the piston on the cylindrical baffle is (16)

$$p(r, \theta, \phi) = \frac{2\rho_f c_f \alpha_0 L_0}{\pi^2 r \sin \theta} J_0(kL_0 \cos \theta) e^{jk(r-L_1 \cos \theta)} \sum_{m=-\infty}^{+\infty} \frac{(-j)^m J_0(m\alpha_0)}{H_m^{(1)'}(kL_0 \cos \theta)} e^{jm(\phi-\alpha_1)} \tag{16}$$

where $2L_0$ and $2\alpha_0$ are the axial length and circumferential angle of the piston, L_1 is the axial distance between the center of the piston and the origin, and α_1 is the azimuth angle of the center of the piston. The local coordinate system of the piston is spherical coordinate system (r, θ, ϕ) , and the origin of the local coordinate system is the intersection of the axis of cylindrical baffle and the perpendicular bisector of the piston, such as O_1 . r, θ and ϕ can be obtained after the location of field point is known. All the parameters are shown in Fig. 4.

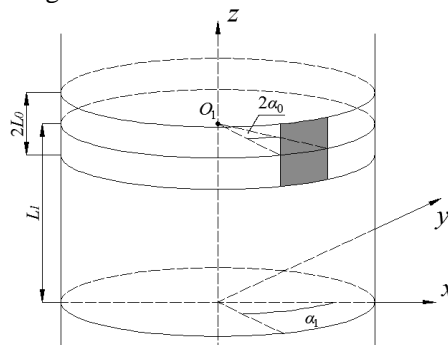


Figure 4 – Cylindrical baffle and the corresponding piston

Once the elements of $[G]$ are calculated by using the Eq. (16) and the velocity are obtained by adopting WBM, the radiated pressure can be easily obtained though Eq. (15).

3. NUMERICAL RESULTS AND DISCUSSION

The vibration and acoustic responses due to point force are presented for a ring-stiffened cylinder of radius $R=3.5\text{m}$, hull thickness $h=0.032\text{m}$, length $L=36\text{m}$, two evenly spaced bulkheads of thickness $h_p=0.032\text{m}$, and end plate thickness $h_e=0.032\text{m}$. The internal stiffeners with rectangular cross-section of $0.025 \times 0.25\text{m}$ are equally spaced by $b=0.6\text{m}$. The material properties for hull, bulkheads and stiffeners are the same, density $\rho=7800\text{kg/m}^3$, Poisson's ratio $\nu=0.3$ and Young's modulus $E=2.1 \times 10^{11}\text{N/m}^2$. The structure damping is introduced using a complex Young's modulus $E=E(1-j\eta)$, where $\eta=0.01$ is the structure damping. The location of point force (x_0, ϕ_0) is $(15, -90^\circ)$, as shown in Fig.3. The location of far field pressure point is $(18, 0^\circ, 1000)$ in cylindrical coordinate system.

For validity of present method, a finite element (FE) model is developed using Ansys for fluid-loaded response and boundary element (BE) model is developed adopting Sysnoise for far field acoustic pressure. In the FE model, the structure, corresponding to a finite cylindrical shell closed by two end plates and two internal bulkheads, are meshed with Shell 63 elements, and stiffeners are meshed with Beam 188 elements. Fluid 30 and Fluid 130 elements are used to simulate the fluid and absorbing boundary around the fluid domain.

3.1 Convergence and validity

The structural response, at particular frequency, is the superposition of the circumferential mode number n , from 0 to infinite, which means numerical calculation need to be truncated. In order to ensure the convergence of results from WBM, Fig. 5 shows the vibration response results of different truncation orders of n . It is observed the results of different truncated orders are excellent identical and the highest order of truncated circumferential mode is 25 in the following analysis.

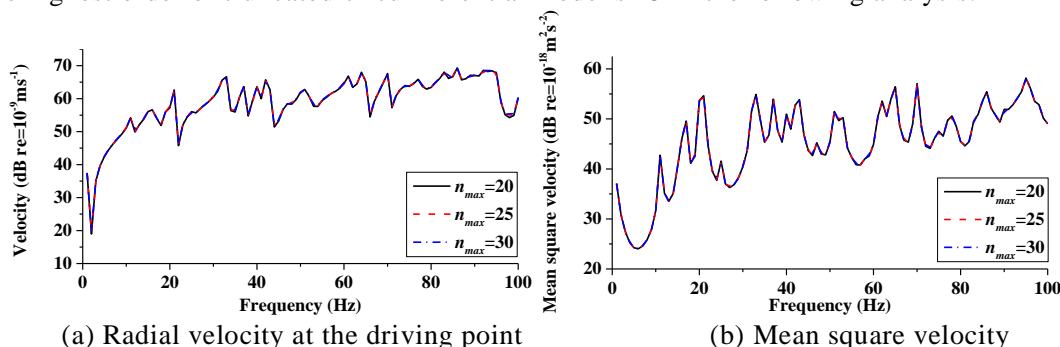


Figure 5 – Convergence analysis of results of WBM

Sec.2.5 discusses the far field response obtained using ERSM, which need dividing the vibrating surface into small elements as many as possible. On the other hand, the computation efficiency decreases rapidly as the number of elements becomes large. Three different meshes, 48×60 , 48×120 and 64×120 (circumferential direction and axial direction, respectively), are used to analyze the convergence of ERSM and they are named Mesh1, Mesh2 and Mesh3, respectively. Fig. 6 compares the predicting results of three kinds of meshes and it is observed the curves are identical. As a result, Mesh2, which achieves high computation efficiency and adequate converged results, is adopted in the following analysis.

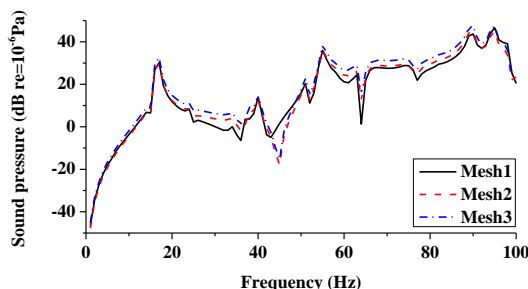


Figure 6 – Acoustic response calculated by three different meshes

Fig.7 compares the structural response calculated by the WBM and FEM. At low frequencies, a good agreement is observed between the results of two methods except for the amplitude of a few

peaks, 33Hz and 42Hz. Taking the step of excitation frequency and the effect of structure damping on structural response into account, the differences may come from the structure damping and become unobvious if the step is small enough. Although the discrepancies become more obvious at higher frequencies, such as the shift of frequencies of peaks, the amplitude of the peaks does not shift significantly. The differences are due to the approximate solutions for the external fluid loading, using the pressure of infinite model to analyze the finite one, and its influence becomes more important as frequency increases. Except for those slight discrepancies, a good match between WBM and FEM is obtained, thus confirming the analytic model of WBM.

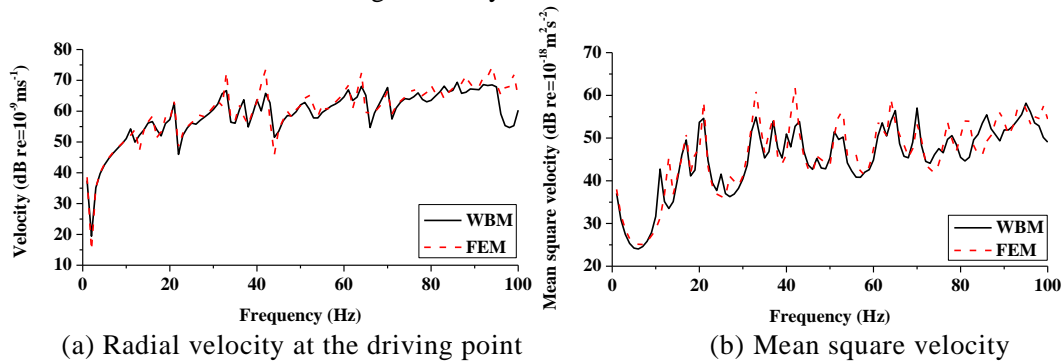


Figure 7 – Comparison of structure response of different methods

Fig. 8 shows the far field sound pressure of different methods. WBM and FEM denote the vibration response is obtained from analytical and computational solution, respectively. ERSM and BEM represent the ATV is calculated by analytical solutions and by means of the Sysnoise, respectively. Comparing the results of the WBM/ERSM and WBM/BEM, a good agreement is observed except for the range from 35Hz to 50Hz, and it can be concluded ERSM is an accuracy method calculating ATV of far field point. Comparing the curves of WBM/ERSM and FEM/BEM, the former of which is the analytical method of present paper and the latter of which is the computational method, it reveals the first peaks of two methods agree well and the differences become obvious as frequency increases but the trend is similar. Taking the results in Fig.7 into account, the differences are mainly attributed to the differences in vibration responses. In general, the present method (WBM/ERSM) is an accurate method in the analysis of vibration and acoustic responses.

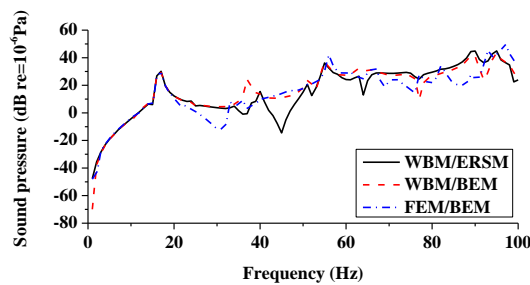


Figure 8 – Comparison of far field sound pressure of different methods

3.2 Effect of the bulkheads

Fig.9 presents the structural and acoustic responses with one, two or five evenly spaced bulkheads. Significant influence of the number of bulkheads on the structural response is observed from Fig. 9(a) and 9(b). As the number of bulkheads increases, the amplitude of velocity with 5 bulkheads, except for some peaks, is obvious lower than the other cases, which is attributed to added stiffness of the increased number of bulkheads. The reason why the amplitudes of some peaks with 5 bulkheads are larger is that the driving point is located at the peaks of mode shape when the axial mode number is odd. Meanwhile, the location of external force with 5 bulkheads is at the nodal line when axial mode number is even and the corresponding modes cannot be excited, which results in the resonant peaks are fewer. Fig. 9(c) shows the far field pressure and it is observed the peaks shift to higher frequencies only at low frequency range as the number of bulkheads increases, but the amplitudes does not shift significantly, which indicates the added stiffness does not affect the transmission of sound into the acoustic field although it reduces amplitude of structural response obviously.

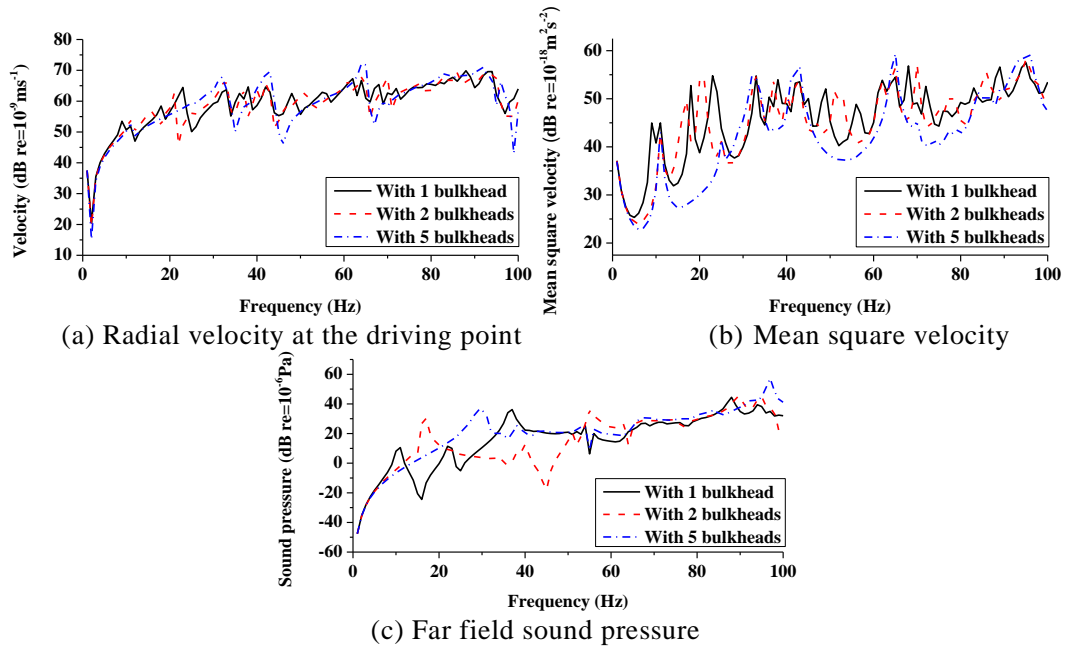


Figure 9 – Effect of the number of bulkheads on the structural and acoustic responses

Fig.10 shows the responses of the three different distributions of bulkheads. Distribution 1 represents the two bulkheads located at 10.8m and 25.2m, Distribution 2 represents the bulkheads evenly spaced, namely located at 12m and 24m, Distribution 3 represents the bulkheads located at 13.2m and 22.8m. Since the differences of the three distributions are not obvious compared with the length of the compartment, the main effect of the distribution of bulkheads is the peaks shift to higher frequencies as the distance of the two bulkheads decreases while the amplitudes of resonant peaks are at the same levels.

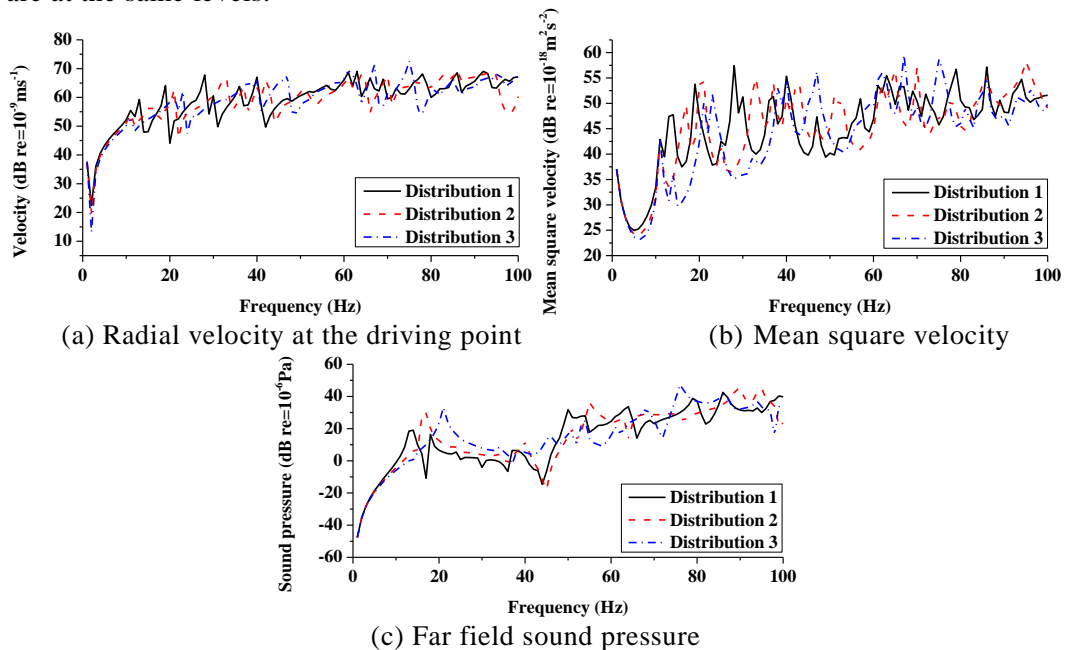


Figure 10 – Effect of distributions of bulkheads on the structural and acoustic responses

The influence of bulkhead thickness on the structural and acoustic responses is presented in Fig.11. It is observed the bulkhead thickness has negligible influence on the vibration and acoustic responses.

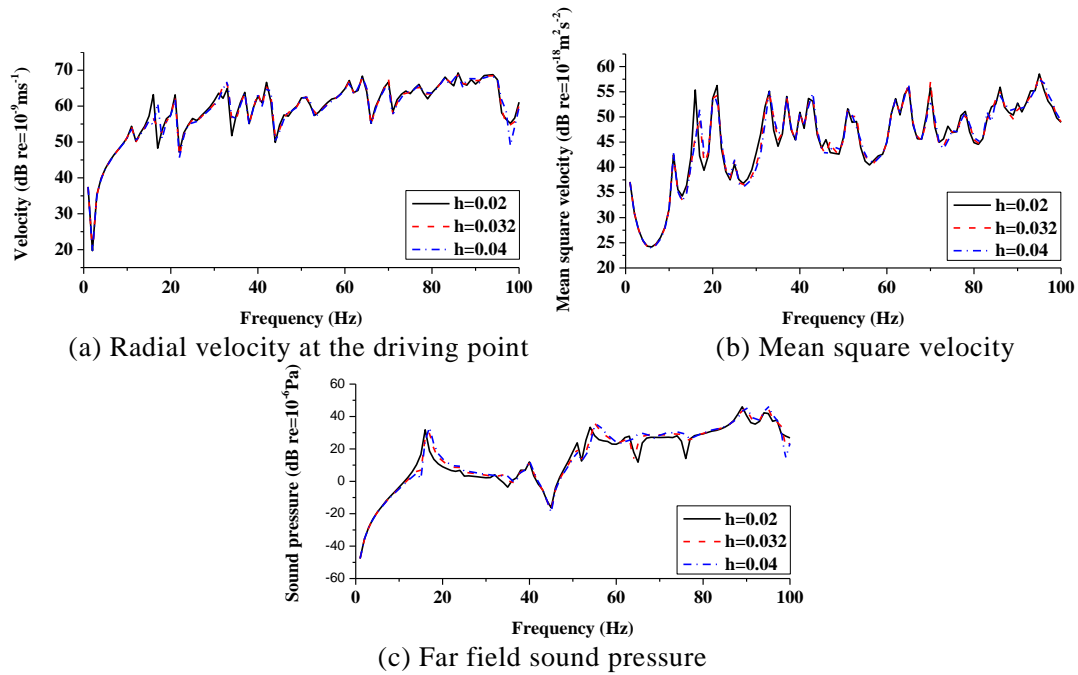


Figure 11 – Effect of bulkhead thickness on the structural and acoustic responses

3.3 Effect of the point force excitation

Fig.12 presents the structure and acoustic response as driving point located at three different points. Case1, Case2 and Case3 denote the axial coordinate of the driving point is 9m, 15m and 18m, respectively. Since the hull is the periodic structure and the locations of forces in Case1 and Case2 are similar corresponding to the bulkhead, the structural and acoustic responses of those two cases agree well. For Case3, the amplitudes of structure response and the sound pressure are obvious larger than others two cases, which is due to the fact the distance between driving point and the bulkhead is the largest. Furthermore, the peaks of structure response in Case3 are fewer than others, which is attributed to the driving point located at the nodal line when the axial mode is even and the corresponding modes cannot be excited.

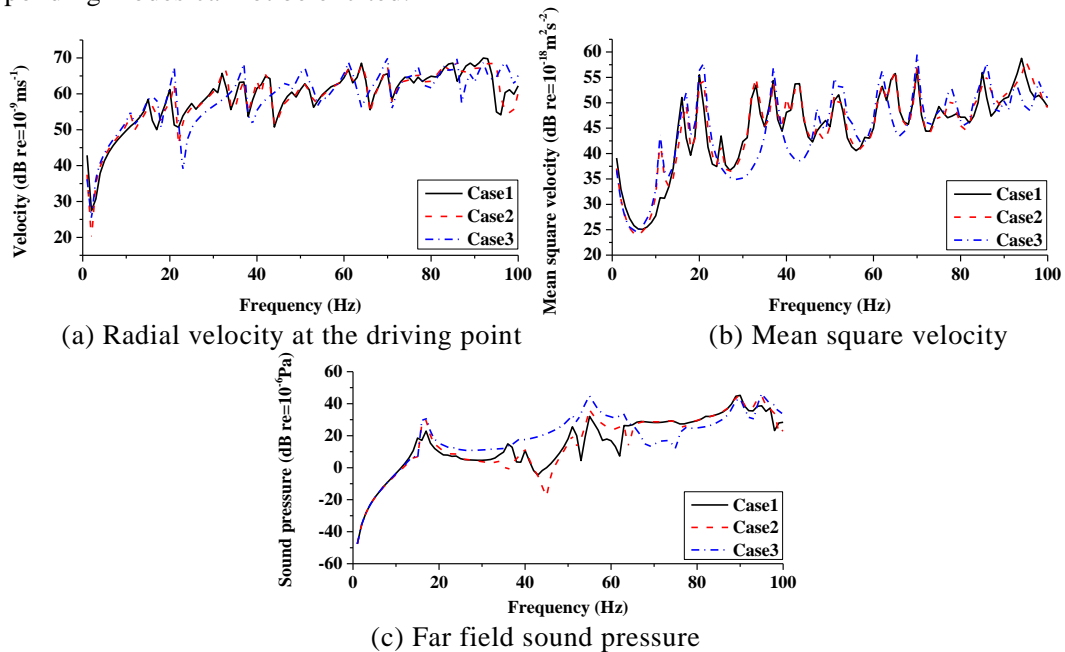


Figure 12 – Effect of driving point on the structural and acoustic responses

4. CONCLUSIONS

An analytic method to predict the vibration and acoustic responses of cylindrical shell with

bulkheads based on wave based method (WBM) has been presented. The stiffened cylindrical shell with bulkheads is divided into different substructures, such as cylindrical shells, annular plates and circular plates. The motion of cylindrical shell is described by Donnell-Mushrari theory and the equations of motion of stiffeners are described by equations of annular plate in contrast to the equations of motion of beam. The dynamic field variables in each substructure are expanded as wave functions. Numerical results show good agreement between analytical and computational results. The influence of various complicating factors on the vibration and acoustic responses to a radial harmonic excitation is discussed. The variation of bulkhead thickness is shown to have negligible influence. Although the amplitude of structure response is significantly reduced by increasing the number of bulkhead, the far field sound pressure is not affected excepting the frequencies of peaks shift to higher frequencies at low frequency range. The distribution of bulkheads mainly affects the resonant frequencies and hardly affects the amplitudes when the length of compartment does not shift obviously. As the locations of different point forces are similar corresponding to the bulkhead in periodic cylindrical shell, the structural and acoustic responses are similar. Furthermore, the larger the distance of driving point and the nearest bulkhead is, the greater the amplitudes of the structural and acoustic responses are.

ACKNOWLEDGEMENTS

All the work in this paper obtains great support from the National Natural Science Foundation of China (51179071).

REFERENCES

1. Thein W, Hu WCL. Vibration analysis of stiffened cylinder including inter-ring motion. *J Acoust Soc Am.* 1967; 43 (5):1005-1016.
2. Basdekas NL, Chi M. Response of oddly stiffened circular cylindrical shell. *J Sound Vib.* 1971; 17(2):187-206.
3. Hoppmann II WH. Some characteristics of the flexural vibrations of orthogonally stiffened cylindrical shells. *J Acoust Soc Am.* 1958; 30 (1):77-82.
4. Caresta M, Kessissoglou NJ. Structural and acoustic responses of a fluid-loaded cylindrical hull with structural discontinuities. *Applied Acoustic.* 2009; 70:954-963.
5. Caresta M, Kessissoglou NJ. Acoustic signature of a submarine hull under harmonic excitation. *Applied Acoustic.* 2010; 71:17-31.
6. Tso YK, Hansen CH. Wave propagation through cylinder/plate junctions. *J Sound Vib.* 1995; 186(3):447-461.
7. Scott JFM. The free modes of propagation of an infinite fluid-loaded thin cylindrical shell. *J Sound Vib.* 1988; 125(2):241-280.
8. Wang C, Lai JCS. The sound radiation efficiency of finite length acoustically thick circular cylindrical shells under mechanical excitation, I: Theoretical analysis. *J Sound Vib.* 2000; 232(2):431-447.
9. Chien CC, Rajiyah H, Atluri SN. An effective method for solving the hypersingular integral equations in 3-D acoustic. *J Acoust Soc Am.* 1990; 88(2):674-679.
10. Jeans RA, Mathews IC. Solution of fluid-structure interaction problems using a coupled finite element and variational boundary element technique. *J Acoust Soc Am.* 1990; 88 (5):2495-2466.
11. Wang B, Tang WL, Fan J. Approximate method to acoustic radiation problems: element radiation superposition method. *Chinese J Acous.* 2008; 27:350-357.
12. Desmet W. A wave based prediction technique for coupled vibro-acoustic analysis. PHD thesis, KU, Leuven, Belgium; 1998.
13. Wei JH, Chen MX, Hou GX, Xie K, Deng NQ. Wave based method for free vibration analysis of cylindrical shells with nonuniform stiffener distribution. *J Vib Acous.* 2013; 135(6): 061011.
14. Flügge W. *Stress in shells.* Berlin, Germany: Springer; 1973.
15. Chen MX, Zhang C, Tao XF, Deng NQ. Structural and acoustic responses of a submerged stiffened conical shell. *Shock and Vibration.* 2014; Volume 2014, Article ID 954253, 14 pages.
16. Junger MC, Feit D. *Sound, structure, and their interaction.* Cambridge Mass, USA: MIT Press; 1986.